https://doi.org/10.5194/angeo-2020-32
Preprint. Discussion started: 26 June 2020

Annales Geophysicae Discussions
Open Access
EGU

Multipoint Observations of Compressional Pc5 Pulsations in the Dayside Magnetosphere and Corresponding Particle Signatures

Galina Korotova[1,2], David Sibeck[3], Mark Engebretson[4], Michael Balikhin[5], Scott Thaller[6], Craig Kletzing[7], Harlan Spence[8], and Robert Redmon[9]

[1]IPST, University of Maryland, College Park, MD, USA
[2]IZMIRAN, Russian Academy of Sciences, Moscow, Troitsk, Russia
[3]NASA/GSFC, Code 674, Greenbelt, MD, USA
[4] Department of Physics, Augburg University, Minneapolis, MN, USA
[5]Department of Automatic Control and Systems Engineering, University of Sheffield, Sheffield, UK.
[6] LASP, University of Colorado, Boulder, CO, USA
[7]Department of Physics and Astronomy, Iowa University, Iowa City, IA, USA
[8]EOS, University of New Hampshire, Durham, NH, USA
[9]Solar and Terrestrial Physics division, NGDC/NOAA, Boulder, CO, USA

Abstract

We use Van Allen Probes Radiation Belt Storm Probes-A and -B (henceforth RBSP-A and -B) and GOES-13 and -15 (henceforth G-13 and G-15) multipoint magnetic field, electric field, plasma, and energetic particle observations to study the spatial, temporal, and spectral characteristics of compressional Pc5 pulsations observed during the recovery phase of a strong geomagnetic storm on January 1, 2016. From ~19:00 UT to 23:02 UT, successive magnetospheric compressions enhanced the peak-to-peak amplitudes of Pc5 waves with 4.5-6.0 mHz frequencies from 0-2 to 10-15 nT at both RBSP-A and -B, particularly in the prenoon magnetosphere. Poloidal Pc4 pulsations with frequencies of ~22-29 mHz were present in the radial Bx component. The frequencies of these Pc4 pulsations diminished with increasing radial distance, as expected for resonant Alfvén waves standing along field lines. The GOES spacecraft observed Pc5 pulsations with similar frequencies to those seen by the RBSP, but Pc4 pulsations with lower frequencies.

Both RBSP-A and -B observed frequency doubling in the compressional component of the magnetic field during the Pc5 waves, indicating a meridional sloshing of the equatorial node over a combined range in Z_{SM} from 0.25 to -0.08 Re, suggesting that the amplitude of this

https://doi.org/10.5194/angeo-2020-32
Preprint. Discussion started: 26 June 2020

Annales Geophysicae Discussions

meridional oscillation was ~0.16 Re about an equatorial node whose mean position was near Z_{SM} = ~0.08 Re. RBSP-A and -B HOPE and MagEIS observations provide the first evidence for a corresponding frequency doubling in the plasma density and the flux of energetic electron, respectively. Energetic electron fluxes oscillated out of phase with the magnetic field strength with no phase shift at any energy. In the absence of any solar wind trigger or phase shift with energy, we interpret the compressional Pc5 pulsations in terms of the mirror mode instability.

Introduction

ULF pulsations with periods of 100s or greater and high azimuthal wave numbers (m) with magnetic field perturbations in the radial direction and electric field perturbations in the azimuthal direction within the Earth's magnetosphere are typically poloidal waves [Sugiura and Wilson, 1964]. According to Elkington et al. [2003], energetic particles with drift frequencies of 6.7-22 mHz and 1.7-6.7 mHz can readily interact with corresponding high-m poloidal Pc4 and Pc5 pulsations. Because the atmosphere and ionosphere screen these high-m waves from the ground, they can only be studied with the help of satellite observations. Thus studies like that of Dai et al. [2013] employed observations from locations at or near geosynchronous orbit. Higbie et al. [1982] and Nagano and Araki [1983] showed that long-lasting compressional Pc5 pulsations occur most frequently in the dayside magnetosphere during the recovery phase of magnetic storms. Storm-time Pc5 pulsations occur in the afternoon sector between 12:00 and 18:00 local time following injections of ring current particles [Kokubun, 1985].

A number of studies have examined compressional Pc5 waves outside geostationary orbit. According to these studies, compressional Pc5 waves were observed in the dawn [Hedgecock, 1976], dusk [Constantinescu et al., 2009] and noon [Takahashi et al., 1985] sectors. Zhu and Kivelson [1991] reported that intense compressional waves are a persistent feature on both flanks of the magnetosphere. Compressional Pc5 pulsations occur within ~20° region of the magnetic equator [Vaivads et al., 2001]. They have several Re wavelengths [Walker et al., 1982] and often exhibit harmonics. Elkington et al. [2003] noted that poloidal and compressional modes are far more effective the radial transport of energetic particles than the toroidal mode. Two methods are used to identify the harmonic mode of a poloidal oscillation. The first compares the phase difference between the radial component of the magnetic field and the azimuthal component of the electric field [Takahashi et al., 2011]. The second compares observed wave frequencies with the eigenfrequencies predicted by theory [Cummings, 1969]. The multi-satellite study of Takahashi et al. [1987a] showed that a compressional Pc 5 wave had an antisymmetric standing structure.

https://doi.org/10.5194/angeo-2020-32
Preprint. Discussion started: 26 June 2020


Annales Geophysicae Discussions

Compressional Pc5 pulsations have been ascribed to numerous excitation mechanisms. They can be produced by internal and external processes. It is supposed that the solar wind is the main external source for pulsations produced by the Kelvin-Helmholtz (KH) instability at the magnetopause or the inner edge of the low-latitude boundary layer [e.g., Guo et al., 2010]. Observations indicating enhanced rates of Pc5 occurrence during periods of greater solar wind velocity support this model [e.g., Engebretson et al., 1998]. Transient variations in the dynamic pressure of the solar wind or foreshock [e.g., Wang et al., 2018; Shen et al., 2018] that cause abrupt changes in the magnetic field strength in the magnetosphere and sudden impulses in the ionosphere [e.g., Zhang et al., 2010, Sarris et al., 2010] provide another possible trigger for Pc5 pulsations. External pressure impulses can cause compressional oscillations of the magnetosphere with discrete eigenfrequencies, known as global modes or cavity/waveguide modes [Samson et al., 1992]. Periodic solar wind dynamic pressure variations directly drive some compressional magnetospheric magnetic field oscillations [e. g., Kepko et al., 2003; Motoba et al., 2003]. Takahashi and Ukhorskiy [2008] considered solar wind pressure variations as the main external driver of Pc5 pulsations observed at geosynchronous orbit in the dayside magnetosphere.

Internal generation mechanisms for compressional Pc5 pulsations include the drift-bounce resonant instability which occurs for particles with resonance drift and bounce periods [Southwood et al., 1969] and the drift-mirror instability in the presence of strong temperature anisotropies [Chen and Hasegawa, 1991]. In high β plasmas (β is the plasma pressure divided by the magnetic pressure), these mechanisms favor antisymmetric waves [Cheng and Lin, 1987].

One of the possible mechanisms of generation of compressional Pc5 pulsations observed at geosynchronous orbit is a drift mirror instability of ring current particles [e.g., Lanzerotti et al., 1969]. While the observed anticorrelated magnetic field strength and ion flux oscillations are expected for a drift mirror wave [Kremser et al., 1981], the instability criterion is generally not satisfied [Pokhotelov et al., 1986]. One possible reason for the lack of consistency between theory and observation might be because the real geometry of the magnetosphere is not taken into account [Cheng and Lin, 1987]. Compressional pulsations are often accompanied by pulsations in particle fluxes [Kremser et al., 1981; Liu at al., 2016]. Particle observations can provide useful information on the spatial and wave structure of ULF pulsations. Lin et al. [1976] explained flux oscillations as the adiabatic motion of particles in a magnetohydrodynamic wave. Kivelson and Southwood [1985] studied charged particle behavior in compressional ULF waves and showed that “a mirror effect” is the dominant cause

https://doi.org/10.5194/angeo-2020-32
Preprint. Discussion started: 26 June 2020


Annales Geophysicae Discussions

for particle flux modulations. Finite gyroradius effects enable detection of gradients in particle flux associated with waves [e.g., Korotova et al., 2013].

1. Objectives

We use multipoint magnetic field, plasma, and energetic particle observations from RBSP-A and -B and G-13 and -15 to study the spatial, temporal, and spectral characteristics of compressional Pc5 pulsations observed deep within the magnetosphere during the recovery phase of the strong magnetic storm which began on December 31, 2015. We investigate the mode of the waves and their nodal structure. We focus on the properties of double frequency pulsations that occurred in the vicinity of the geomagnetic equator. We demonstrate that the energetic particles respond directly to the compressional Pc5 pulsations and also exhibit a double frequency oscillation. We search for possible solar wind triggers and test two possible generation mechanisms: drift-bounce resonance, and mirror instability. The paper is organized as follows: Section 2 describes instruments and resources. Section 3 presents the solar wind and IMF conditions. Section 4 provides an analysis of these waves and their generation mechanisms.

2. Resources

The Van Allen Probes mission can be used to study the geospace response to a fluctuating solar wind. The mission began in August 2012 with a twin spacecraft launch into similar 10° inclination orbits with perigee altitudes slightly greater than 600 km and apogee altitudes just beyond 30000 km [Mauk et al., 2012]. The spacecraft carry instruments that measure electromagnetic fields, waves, and charged particle populations deep within the magnetosphere. This paper employs observations of 20-4000 keV electrons from the MagEIS instrument [Blake et al., 2013] in the Energetic Particle, Composition, and Thermal (ECT) suite [Spence et al., 2013] in conjunction with observations from the magnetometer in the Electric and Magnetic Field Instrument Suite and Integrated Science suite [Kletzing et al., 2013], and the Electric Field and Waves (EFW) [Wygant et al., 2013] instrument. We examine electric and magnetic field measurements with 11s and 4s time resolution, respectively, and differential particle flux observattions with ~11s (spin period) time resolution. The data are provided by NASA/GSFC's CDAWEB in the MGSE (modified GSE) coordinate system. We use magnetic field data from G-13 and -15 with 0.5 s time resolution [Singer et al., 1996]. Finally, we employ Wind solar wind magnetic field and 3DP plasma data with 3s time resolution [Lepping et al., 1995; Lin et al., 1995].

https://doi.org/10.5194/angeo-2020-32
Preprint. Discussion started: 26 June 2020

Annales Geophysicae Discussions

3. Orbits and solar wind and geomagnetic conditions

The pulsation events to be studied here occurred late on January 1, 2016, following a prolonged period of strongly southward IMF orientation and geomagnetic activity. A substantial increase in the solar wind dynamic pressure early on December 31 was followed by a strong southward IMF that persisted almost without interruption from 11:00 UT on December 31, 2015 until 09:00 UT on January 1, 2016 (not shown). Figure 1 shows geomagnetic activity indices Dst, Kp and AE obtained from the OMNI database for the three day interval from 12:00 UT on December 30, 2015 to 24:00:00 UT on January 1, 2016. A strong electrojet with AE index greater than 2100 nT at 12:36 UT on December 31, 2015 was followed by two moderate substorms that enhanced AE at ~14:00 and 18:45 UT on January 1, 2016. The Dst index responded by reaching a value as low as -110 nT at 00:30 UT on January 1, 2016. Shading highlights the interval from ~18:55 to 23:02 UT late in the recovery phase and late in the day on January 1, 2016 when the Van Allen Probes and GOES spacecraft observed the strong compressional Pc5 pulsations of interest to this study.

The latter interval was marked by strong variations in the solar wind dynamic pressure. Figure 2 presents Wind observations of the magnetic field and plasma from 16:00 to 24:00 UT on January 1, 2016, during which time the spacecraft moved from GSM (X, Y, Z) = (194.7, 20.1, -12.5) Re to (194.8, 23.6, -7.4) Re. Shading marks an interval of depressed magnetic field strengths and generally anticorrelated enhanced densities, velocities and solar wind dynamic pressures. The cone angle was less than 45^0 during this interval. The magnetic field was briefly aligned with the Sun-Earth line (Bx) at the center of the interval from 20:00-21:00 UT. For most of the ~4h long shaded interval, IMF Bx (By) was predominantly positive (negative) and the Bz component remained almost constant near 0 nT, indicating a spiral and equatorial IMF configuration.

Figure 3 presents RBSP-A and -B and G-13 (MLT~ UT-5) and -15 (MLT~ UT- 9) trajectories from 15:00 UT to 24:00 UT on January 1, 2016 in the X-Y and X-Z GSM planes. Open circles mark the beginning of the spacecraft trajectories which are duskward for the GOES spacecraft and duskward at apogee for the Van Allen Probes. All of the spacecraft were north of the equator when in the dayside magnetosphere. The thick line segments (dots) indicate the locations of the spacecraft at the times when (weak) Pc5 magnetic field pulsations occurred.

Figure 4 compares lagged Wind solar wind dynamic pressure variations with G-13 and -15 observations of the dayside magnetospheric magnetic field. The arrows connect enhancements of the solar wind dynamic pressure to corresponding compressions of the magnetosphere. It is relatively easy to associate the GOES magnetic field enhancements with

https://doi.org/10.5194/angeo-2020-32
Preprint. Discussion started: 26 June 2020


Annales Geophysicae Discussions

corresponding features in the solar wind dynamic pressure at the beginning and the end of the interval but less easy from 19:50 UT to 21:20 UT corresponding to ~ 20:45 UT and 22:15 UT at the GOES spacecraft. The lag time from Wind to the Earth is not uniform and depends on IMF orientation. At the beginning and end of the interval, when the IMF was spiral (Bx >0, By <0), the lag was in the range of ~46 to 58 min. Consistent with expectations, the lag became greater for the interval from ~ 19:50 UT to 21:20 when the IMF was nearly radial (By and Bz ~0 nT). The reasonable correspondence of the magnetosphere compressions to solar wind dynamic pressure variations demonstrates that Wind was a good monitor for solar wind conditions and that a series of pressure enhancements were applied to the magnetosphere during the interval of interest. Pc5 pulsation amplitudes at G-13 and -15 were greater during the interval of enhanced solar wind dynamic pressure and magnetospheric magnetic field strengths than they were at earlier and later times.

4. Pulsation Observations

4.1. Spatial characteristics of Pc5 pulsations

Consider the spatial extent, temporal, and spectral characteristics of the compressional Pc5 pulsations. Figure 5 shows RBSP-A (a) and -B (b) magnetic field observations in GSM coordinates from 18:40 UT to 21:10 UT and from 20:40 UT to 23:10 UT, respectively, on January 1, 2016. Taken together, the RBSP-A and -B observed compressional Pc5 pulsations that occupied the inner dayside magnetosphere from 5.26 to 5.75 R_E and from 09:56 to 12:44 MLT. Prior to the arrival of the strong solar wind dynamic pressure variations, RBSP-A observed very weak compressional pulsations with Pc5 periods and amplitudes of 1-3 nT from 18:15 to 18:55 UT. After G-15 began to observe compressions at about 19:00 UT (Figure 4), the amplitudes of the pulsations at RBSP-A began to increase (Figure 5). They increased prominently to values ranging from 10 to 15 nT in the Bz component with the peak amplitudes occurring prior to local noon. The Bz component oscillated out of phase with the Bx component and in quadrature with the By component. The compressional pulsations at RBSP-A ended at 20:58 UT. RBSP-B observed similar compressional Pc5 pulsations from 20:46 UT that ceased simultaneously with the end of the magnetospheric compression seen by G-15 about 23:02 UT.

Figure 6 shows G-13 and -15 observations of the magnetic field in GSM coordinates from 18:00 UT to 24:00 UT. The spacecraft observed long-duration compressional Pc5 pulsations over a wide longitudinal region in the pre- and post-noon magnetosphere from 10:00 to 15:20 MLT (Figure 3). There was also weak preexisting Pc5 wave activity before the strong solar wind dynamic pressure variations. G-15 observed pulsations with amplitude less than 5 nT

https://doi.org/10.5194/angeo-2020-32
Preprint. Discussion started: 26 June 2020


Annales Geophysicae Discussions

from 18:28 UT to 19:04 UT. Then after the subsequent magnetospheric compressions their amplitude increased to values ranging from 10 to 16 nT with peak amplitudes prior to local noon as for the Pc5 pulsations observed by RBSP-A and -B. G-13 observed weak Pc5 pulsations with amplitudes of 2-4 nT throughout most of the time interval from 16:40 UT to 21:00 UT. During the interval from 19:34 UT (~14:45 MLT) to 20:10 UT (~15:20 MLT), the pulsations reached slightly stronger amplitudes of 5-8 nT. At 23:02 UT all wave activity observed at GOES stopped.

We converted the magnetic field observations from GSE into field-aligned coordinates (FAC). Here the Z axis lies parallel to the locally-averaged magnetic field. The Y axis points approximately azimuthally eastward and is transverse to B and to the outward radius vector. The X axis completes the right-handed system and is directed approximately radially outward from Earth. Figure 7 presents RBSP-A and -B magnetic field observations in FAC. The Bz component reached 15 nT and it is the strongest one as is characteristic of compressional pulsations. The amplitudes of the Bx and Bz components are weaker than those of the Bz component and did not exceed 7 nT. Simultaneous RBSP-A and -B electric and magnetic field measurements provide an opportunity to study the structure of the Pc5 waves. Determining the harmonic mode of the Pc5 waves requires us to consider the phase of the azimuthal component of the electric field Ey with respect to the radial component of the magnetic field Bx as a function of latitude [Takahashi et al., 2011]. Figure 8 shows that the phase of the Ey component leads that of the Bx component by 90° at RBSP-A from 19:10 UT to 20:00 UT and therefore the Pc5 waves are second harmonic in nature.

4.2. Spectral characteristics

We calculated dynamic spectra for the magnetic field pulsations. Figure 9 presents the radial, azimuthal and compressional components of the dynamic spectra of the magnetic field at RBSP-A and -B from 18:00 to 21:10 UT and from 20:00 UT to 23:10 UT on January 1, 2016, respectively. The color bar on the right shows the scale for power for frequencies ranging from 0 to 41 mHz in each component. The magnetic field exhibited several wide-band enhancements at frequencies ranging from 4 to 29 mHz. As expected for compressional Pc5 pulsations, both spacecraft observed the strongest power densities in the Bz component at dominant frequencies of ~4.5-6 mHz. Red arrows in the Bz panels of Figure 9 for RBSP-A and -B indicate the double frequency pulsations at ~5.5 mHz and ~11 mHz. We calculated Fourier spectra for the three components of the RBSP-A and -B magnetic field in 600 second sliding-averaged mean FAC for each thirty min interval during the event. Figure 10 presents examples of Fourier spectra

https://doi.org/10.5194/angeo-2020-32
Preprint. Discussion started: 26 June 2020

calculated for the RBSP-A and -B magnetic field from 19:30 UT to 20:00 UT and from 22:30 UT to 23:00 UT, respectively, on January 1, 2016. The red arrows show the dominant frequencies at 5.5 and 5 mHz observed at the two spacecraft, corresponding to periods of 170-200 s. RBSP-A and -B were situated three hours in local time apart, the similar frequencies indicate that conditions in the dayside magnetosphere remained steady for a long time and over a broad region.

In passing, we note the presence of Pc4 pulsations. Returning to Figure 9, we see enhanced power densities at frequencies of ~22-29 mHz with dominant frequencies from 23 to 27 mHz primarily in the radial Bx component. These can be ascribed to poloidal Pc4 produced simultaneously with the Pc5 but likely with another energy source. The frequencies of the Pc4 pulsations decrease with increasing radial distance, as expected for resonant standing Alfvén waves [Sugiura and Wilson, 1964]. Pulsation periods depend upon the magnetic field line length, the magnetic field magnitude, and the ion density**.** Shorter field line lengths and enhanced magnetic field strengths closer to Earth decrease pulsation periods. Blue arrows in Figure 9 indicate Pc4 pulsations at ~25-27 mHz.

Figure 11 presents dynamic spectra for the G-13 and -15 magnetic field in FAC from 18:00 UT to 24:00 UT on January 1, 2016. Spectral power was calculated for frequencies from 0 to 48 mHz. Like the RBSP-A and -B magnetic field spectra, there are two broad frequency band enhancements corresponding to Pc4 and 5 frequencies. The dominant frequencies for the compressional Pc5 pulsations occur from 4.5 to 6.5 mHz. These frequencies are similar to those observed by Van Allen Probes and we suppose that they were generated by the same sources. The Pc4 pulsations are most pronounced in the radial Bx component and display strongest spectral power densities in the frequency range from 13 to 21 mHz. These frequencies are lower than those observed by Van Allen Probes, as expected since the GOES spacecraft were located further radially outward from Earth [Sugiura and Wilson, 1964]. The frequencies of the long-lasting Pc4 pulsations observed by G-15 depended on local time. They decreased from 20-22 mHz in the prenoon magnetosphere to 14-17 mHz near local noon, perhaps in response to differing conditions (e.g., densities). Takahashi at el. [1984] noted that an increase in plasma mass density from morning to afternoon is typical at geosynchronous orbit. Since the frequencies of the Pc4 pulsations depended on local time and radial distance from Earth, their sources must be more localized than those for the Pc5 pulsations.

https://doi.org/10.5194/angeo-2020-32
Preprint. Discussion started: 26 June 2020


Annales Geophysicae Discussions

4.3. Particle signatures

Energetic particle observations provide further information concerning this event. We inspected RBSP-A and -B MagEIS observations of energetic particles from 18:30 UT to 21:00 UT and from 20:40 UT to 23:10 UT on January 1, 2016, respectively, and found that the intensities of electrons with energies from tens of keV to 2 MeV oscillated with Pc5 periods corresponding to those of the magnetic field. Figure 12 shows these oscillations. The energetic electron fluxes oscillated out of phase with the magnetic compressional component of Pc5 pulsations and did not display any phase differences across all energies. The depth of modulation (the peak to valley ratio) is larger for higher energy electrons consistent with the results of Liu et al. [2016] who interpreted similar observations in terms of mirror mode waves. Kivelson and Southwood [1985] noted that the maintenance of pressure balance in low-frequency compressional waves usually requires the presence of some pitch angle anisotropy and the antiphase relation between P and B suggests that particle pitch angle distributions peak near 90°. Figure 13 presents RBSP-A and -B observations of pitch angle distributions for electrons with energies from 54 keV to 1060 keV from 18:30 to 21:00 UT and from 20:40 UT to 23:10 UT on January 1, 2016, respectively. The figure confirms that pitch angle distributions. peak near 90°. Furthermore, it shows that the electron intensities display quasi-periodic enhancements at all energies with the strongest at pitch angles near 90°.

4.4. Double-frequency pulsations

When RBSP-A and -B and G-15 were in the vicinity of the geomagnetic equator the compressional Pc5 pulsations displayed peculiar features indicating frequency doubling. Here the compressional components oscillated with a frequency double that for the transverse components. Coleman [1970] was the first to report observations of such events in the geosynchronous magnetic field. Higuchi et al. [1986] called them harmonic structures when the first and second harmonics exhibited similar amplitudes and transitional structures when the amplitudes of the alternating peak were different. Takahashi [1987b] interpreted double-frequency oscillations in terms of a model invoking the second harmonic structure of an antisymmetric standing wave in which the location of the equatorial node of field-lined displacement oscillates in phase with the wave. Cheng and Qian [1994] presented a model for the magnetic field perturbations during the pulsations reported by Takahashi et al. [1987a, 1990]. Figure 6 in the paper of Korotova et al. [2013] illustrates how low-latitude spacecraft can observe two magnetic field strength enhancements per wave cycle when the equatorial node oscillates up and down in phase with an antisymmetric compressional wave. Right at the equator

https://doi.org/10.5194/angeo-2020-32
Preprint. Discussion started: 26 June 2020


Annales Geophysicae Discussions

the spacecraft observes identical amplitudes for the two compressions. At any other latitude the two compressions at the spacecraft will have different magnitudes and the imbalance between them increases when the spacecraft moves farther from the equator. Takahashi et al. [1997b] showed that that a latitudinal shift of a fraction of degree can turn the harmonic structure of Bz into nonharmonic. Spacecraft located from the magnetic equator at a large distance do not observe frequency doubling, just a single enhancement. Korotova et al. [2013] derived the latitudinal structure of the waves by invoking north-south sloshings of the low-latitude node.

Figure 14 presents (a) RBSP-A and -B observations of double frequency magnetic pulsations and (b) their locations in the X-Y GSM and X-Z SM planes. Dashed lines in Figure 14 indicate intervals when the double frequency pulsations in Bz are most prominent: 20:45-20:54 UT at RBSP-A and 21:03 UT to 21:31 UT at RBSP-B. However, the amplitudes of the second harmonic are generally much lower than those of the first harmonic. At these times, e.g. from 20:05 to 20:45 UT at RBSP-A and 21:35-21:55 UT at RBSP-B, the second harmonic compressions in Bz are barely perceptible. Model predictions for the magnetic field perturbations associated with an equatorial node whose latitude oscillates in phase with an antisymmetric poloidal wave indicate that the ratio of the amplitudes of the first to second harmonic compressions should change with latitude, being ~1 at the average position of the low-latitude node and ~0 at and beyond the maximum latitude to which the oscillating node can reach [Takahashi et al., 1987b]. To determine the meridional motion of the magnetic field node we measured amplitudes of the first and second harmonics of the compressional pulsations. We found that RBSP-A observed ratios near 1 at Z_{SM} = ~0.08 Re while RBSP-B observed ratios near 1 at Z_{SM} = ~0.10 Re. These are the locations where the southward-moving spacecraft pass through the mean positions of the equatorial node. Figure 14a shows that RBSP-A observed second harmonics from Z_{SM} = 0.25 to 0.04 Re, while RBSP-B observed them from Z_{SM} = 0.19 to -0.08 Re. Consequently, we believe that the equatorial node oscillated with an amplitude of at least 0.15 to 0.18 Re. Note however, that the ratio of the first to second harmonics does not show a smooth transition as the spacecraft move equatorward. Either the amplitude of the compressional pulsation or the meridional oscillation in the equatorial node varied in time, probably abruptly.

Figure 12 shows that the compressional pulsations modulated energetic electrons observed by RBSP- A and - B and we should therefore expect to find the signatures of the double-frequency pulsations not only in the magnetic field but also in the fluxes of particles. Takahashi et al. [1990] reported AMPTE/CCE observations of compressional Pc5 pulsations that demonstrated harmonically related transverse and compressional magnetic oscillations that

https://doi.org/10.5194/angeo-2020-32
Preprint. Discussion started: 26 June 2020


Annales Geophysicae Discussions

modulated the flux of medium energy protons (E > 10 keV) with double frequency but did not discuss the event in detail. We report the first evidence for meridional sloshing of the equatorial node in the simultaneous compressional Pc5 pulsations and variations of electrons fluxes and electron densities observed by MagEIS and Hope, respectively. Figure 15 presents RBSP-A (left panel) and -B (right panel) electron fluxes for energies at 31.9 keV and 54.8 keV, electron densities and the Bz component of the magnetic field in FAC from 19:00 UT to 21:00 UT and at RBSP-B from 20:46 UT to 22:10 UT. The panels in the bottom of Figure 15 present expanded views of 20 min intervals with the double-frequency pulsations. The Bz component of the magnetic field varies with double frequencies out of phase with the fluxes of electrons and densities. This study gives better insight into the nodal structure of the waves and helps to clarify their source.

4.5. Testing Pc4-5 pulsation generation mechanisms

We tested several causes for the Pc4-5 pulsations, including solar wind pressure pulses, the KH instability on the magnetopause, drift-bounce resonant particle interactions, and the mirror-mode instability. First, with the exception of the interval from 19:35 UT to 19:55 UT, the Wind observations shown in Figure 2 provide no evidence for periodic solar wind drivers in the Pc5 range, be they density variations or IMF fluctuations, thus ruling out solar wind pressure pulses as the direct cause of the Pc4-5 pulsations. We then considered the possibility of KH waves. These waves are expected when the solar wind velocity is high and both the magnetosheath and magnetospheric magnetic fields lie transverse to the magnetosheath flow, i.e. on the flanks of the magnetosphere when the IMF points southward or in particular northward [e.g., Guo et al., 2010]. As shown in Figure 2, the solar wind velocity during the interval when the Pc5 events occurred was only moderate, 400-450 km/s. Furthermore, the IMF did not point either strongly northward or southward. Therefore, we conclude like many previous researchers that the compressional Pc5 pulsations were excited by processes internal to the magnetosphere.

Southwood [1981] and Kivelson and Southwood [1985] described how the resonant drift-bounce interaction of particles with an azimuthally-propagating wave generates large amplitude ULF waves in an inhomogeneous background field. For this to happen, the wave frequency ω must satisfy the resonance condition:

$$\omega - m\omega_d - N\omega_b = 0, \qquad (1)$$

where ω_d and ω_b are the angular drift and bounce frequencies, N is an integer, and m is the azimuthal wave number. Southwood [1973] predicted that particle flux oscillations just above

https://doi.org/10.5194/angeo-2020-32
Preprint. Discussion started: 26 June 2020

Annales Geophysicae Discussions

and below the resonant energy should be 180° out of phase. As Figure 12 demonstrates, RBSP-A and -B ion and below electron observations provide no evidence for any such phase reversal at any relevant energy. We exclude the drift-bounce resonance as the cause of the compressional Pc5 pulsations.

Finally, we examined the mirror instability criterion. The mirror instability is a kinetic phenomenon that occurs spontaneously in anisotropic high β plasmas when the ratio of perpendicular to parallel pressures is large [Southwood and Kivelson, 1993]. The test for the mirror instability is approximately:

$$\Gamma = 1 + \beta_{\perp} [1 - T_{\perp}/T_{//}] < 0, \qquad (2)$$

where $T_{//,\perp}$ are the plasma temperatures parallel and perpendicular to the ambient magnetic field and $\beta_{\perp}$ is the ratio of the perpendicular component of the thermal plasma pressure to the magnetic pressure. For our calculations we obtained the magnetic field data from EMFISIS and thermal plasma pressures perpendicular and parallel to the magnetic field from RBSPICE. We used the density and temperature from HOPE to calculate the parallel and perpendicular thermal pressures within the energy range covered by this instrument, but found these pressures to be small compared to those from RBSPICE. Consequently, our calculations neglect the contributions from HOPE to the thermal pressures.

Figures 16a and b show RBSP-A and -B plasma and magnetic field parameters characterizing the pulsations. The upper panels indicate that magnetic field and plasma pressures vary in antiphase during the Pc5 pulsations. However, the total pressure is not balanced as might be expected for mirror mode waves. We suppose that this is because the RBSPICE (or even the RBSPICE + HOPE) plasma instruments do not observe the entire plasma distribution. Assuming that the total plasma pressure is proportional to the fraction that RBSPICE does observe, we scaled the thermal plasma pressures observed by RBSPICE upward to values that cause the sum of the magnetic and perpendicular thermal plasma pressure variations associated with the waves to be approximately constant during the intervals from 19:03 UT to 19:14 UT for RBSP-A and from 22:32 UT to 22:56 UT for RBSP-B. The upward scaling factors were 1.97 and 1.69, respectively. We then applied these factors to both the perpendicular and parallel pressures. The third panels of Figures 16a and b show the values of $\beta_{\perp}$ calculated from these scaled pressures. Shaded grey areas in the fourth panels show when the drift mirror instability is satisfied (< 0). As the test for the mirror instability is satisfied throughout most of the intervals of enhanced temperature (pressure) anisotropy and $\beta > 1$ at RBSP-A and -B, we attribute the compressional Pc5 pulsations observed on January 1, 2016 to the mirror instability.

https://doi.org/10.5194/angeo-2020-32
Preprint. Discussion started: 26 June 2020


Annales Geophysicae Discussions

401

402 **Conclusions**

403 We used Van Allen Probes and GOES multipoint magnetic field, electric field, plasma
404 and energetic particle observations to study the nature of compressional Pc5 pulsations at the end
405 of a strong magnetic storm on January 1, 2016. From ~ 19:00 UT to 23:02 UT the
406 magnetosphere was compressed and transient increases of the total magnetic field strength
407 occurred every 20-40 min. During this interval the spacecraft observed compressional Pc 5
408 pulsations over a large longitudinal extent. They occupied the dayside magnetosphere from 5.26
409 to 6.6 Re and from 09:56 to 15:20 MLT. The subsequent solar wind pressure increases and
410 magnetospheric compressions enhanced the amplitude of Pc5 wave activity to values from 10 to
411 16 nT. The strongest amplitudes occurred prior to local noon. They were observed when the
412 IMF cone angle was less than 45^{o}. We studied the wave mode of the Pc5 pulsations and found
413 that they had an antisymmetric structure.

414 The greatest spectral power densities observed at RBSP-A and -B occurred in the
415 north/south, or Bz, component of the magnetic field at frequencies of ~4.5-6.0 mHz. The two
416 spacecraft observed similar frequencies, indicating that conditions within the dayside
417 magnetosphere remained steady for a long time and over a broad region. Enhanced spectral
418 power densities at frequencies of ~22-29 mHz in the radial Bx component can be attributed to
419 the simultaneous generation of poloidal Pc4 pulsations by a different mechanism. The
420 frequencies of the Pc4 pulsations diminished with increasing radial distance. The dominant
421 frequencies for the compressional Pc5 pulsations observed by GOES resembled those observed
422 by RBSP-A and -B and we suppose that they were generated by the same sources. The Pc4
423 pulsations displayed frequencies that were
424 lower than those observed by RBSP-A and -B, as expected since the GOES spacecraft were
425 located further radially outward from Earth. Since the frequencies of the Pc4 pulsations
426 depended on local time and radial distance from Earth, their sources must be more localized than
427 those for the Pc5 pulsations.

428 When the spacecraft were in the vicinity of the geomagnetic equator, RBSP-A observed
429 meridional sloshing of the equatorial wave node from Z_{SM} = 0.25 to 0.04 Re, while RBSP-B
430 observed them from Z_{SM} = 0.19 to -0.08 Re. Consequently, we believe that the motion of the
431 meridional oscillation of the position of the equatorial node was at least 0.15 to 0.18 Re. We
432 found that RBSP-A observed ratios near 1 at Z_{SM} = ~0.08 Re while RBSP-B observed ratios near
433 1 at Z_{SM} = ~0.10 Re. These were the locations where the southward-moving spacecraft RBSP-A
434 and -B passed through the mean positions of the equatorial node at Z_{SM} = ~0.08 Re and at Z_{SM} =

https://doi.org/10.5194/angeo-2020-32
Preprint. Discussion started: 26 June 2020

Annales Geophysicae Discussions
Open Access
EGU

435 ~0.10 Re, respectively. We report the first evidence for meridional sloshing of the equatorial
436 node in the double-frequency variations of electrons fluxes and electron density observed by
437 MagEIS and HOPE, respectively.

438 The energetic particles observed by RBSP-A and -B exhibited a regular periodicity over a
439 broad range of energies from tens of eV to 2 MeV with periods corresponding to those of the
440 compressional component of the ULF magnetic field. The electron intensities exhibited quasi-
441 periodic enhancements at all energies with the most intense at pitch angles near 90°. The
442 energetic electron fluxes oscillated out of phase with the magnetic field and did not display any
443 phase shift across all energies. The depth of modulation was larger for higher energy electrons.
444 We searched for possible solar wind triggers and discussed generation mechanisms for the
445 compressional Pc5 pulsations in terms of drift mirror instability and drift bounce resonance. We
446 interpret the compressional Pc5 waves in terms of drift-mirror instability.
447
448
449

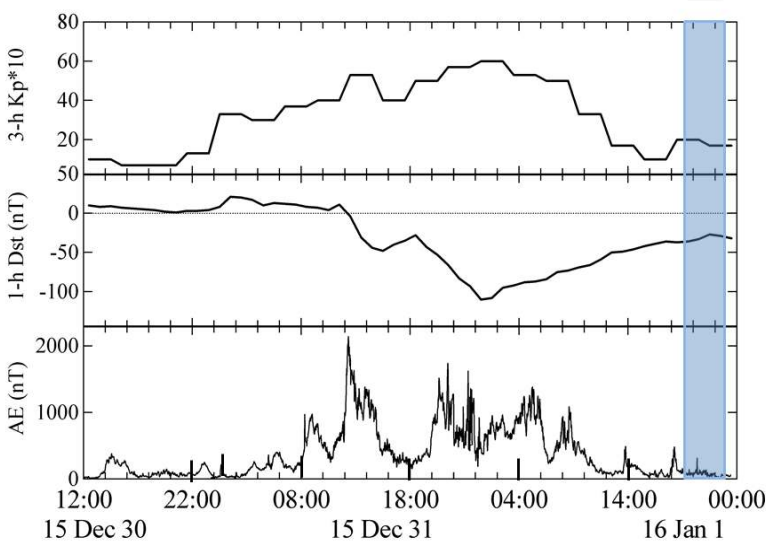

450
451 Figure 1. Geomagnetic activity indices Kp, Dst and AE indices from 12:00 UT on December 30
452 to January 2, 2016 available from the OMNI database (http://omniweb.gsfc.nasa.gov). The
453 shading highlights the interval when the spacecraft observed Pc5 compressional pulsations.
454
455

https://doi.org/10.5194/angeo-2020-32
Preprint. Discussion started: 26 June 2020

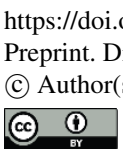

Annales Geophysicae Discussions
Open Access
EGU

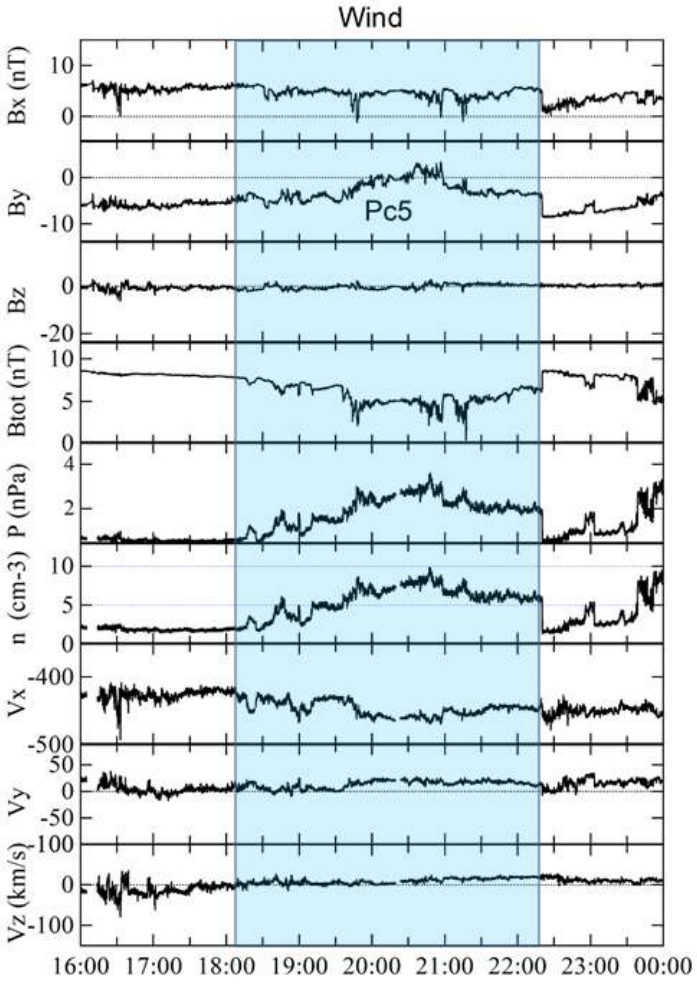

456

457 Figure 2. Wind observations of the magnetic field and plasma from 16:00 UT to 24:00 UT on

458 January 1. 2016. Shading highlights the interval of interest.

459

https://doi.org/10.5194/angeo-2020-32
Preprint. Discussion started: 26 June 2020

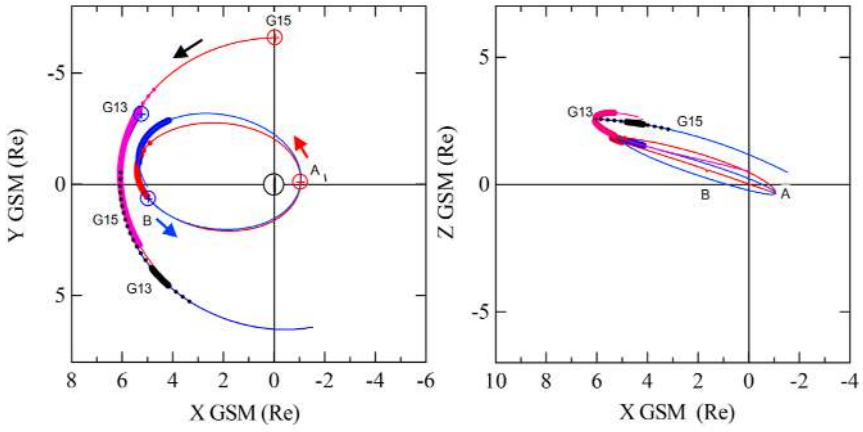

Figure 3. Trajectories of RBSP-A (red) and -B (blue) and G-13 (blue) and -15 (red) from 15:00 UT to 24:00 UT on January 1, 2016 in the X-Y and X-Z GSM planes. Open circles mark the beginning of the spacecraft trajectories, that are duskward in the dayside magnetosphere. The thick line segments indicate the locations of the spacecraft at the times when compressional Pc5 magnetic field pulsations occurred. Dots mark their locations where weak pulsations (A < 5 nT) occurred.

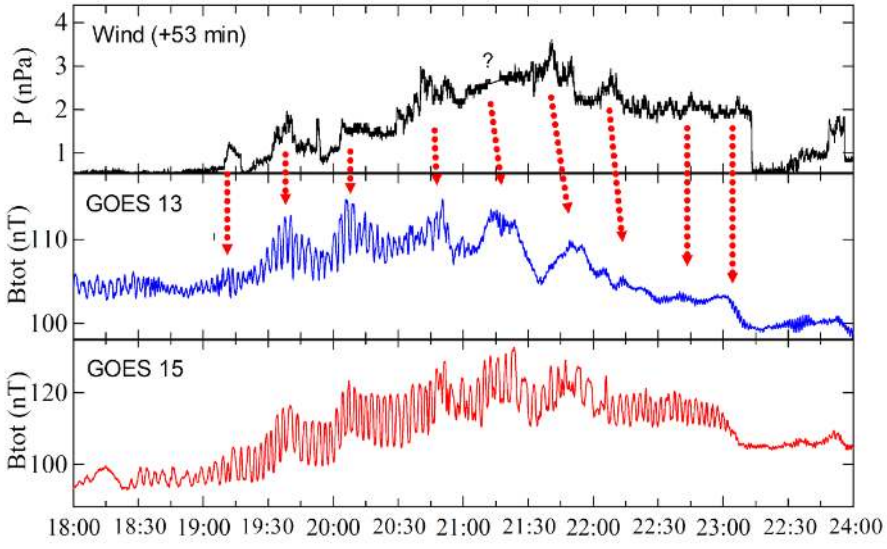

Figure 4. Observations of the solar wind dynamic pressure at Wind (time shifted) and the total magnetic field strength at G-13 and -15 from 18:00 UT to 24:00 UT. The arrows connect

https://doi.org/10.5194/angeo-2020-32
Preprint. Discussion started: 26 June 2020

Annales Geophysicae Discussions
Open Access
EGU

471 enhancements of the solar wind dynamic pressure to corresponding compressions of the
472 magnetosphere.

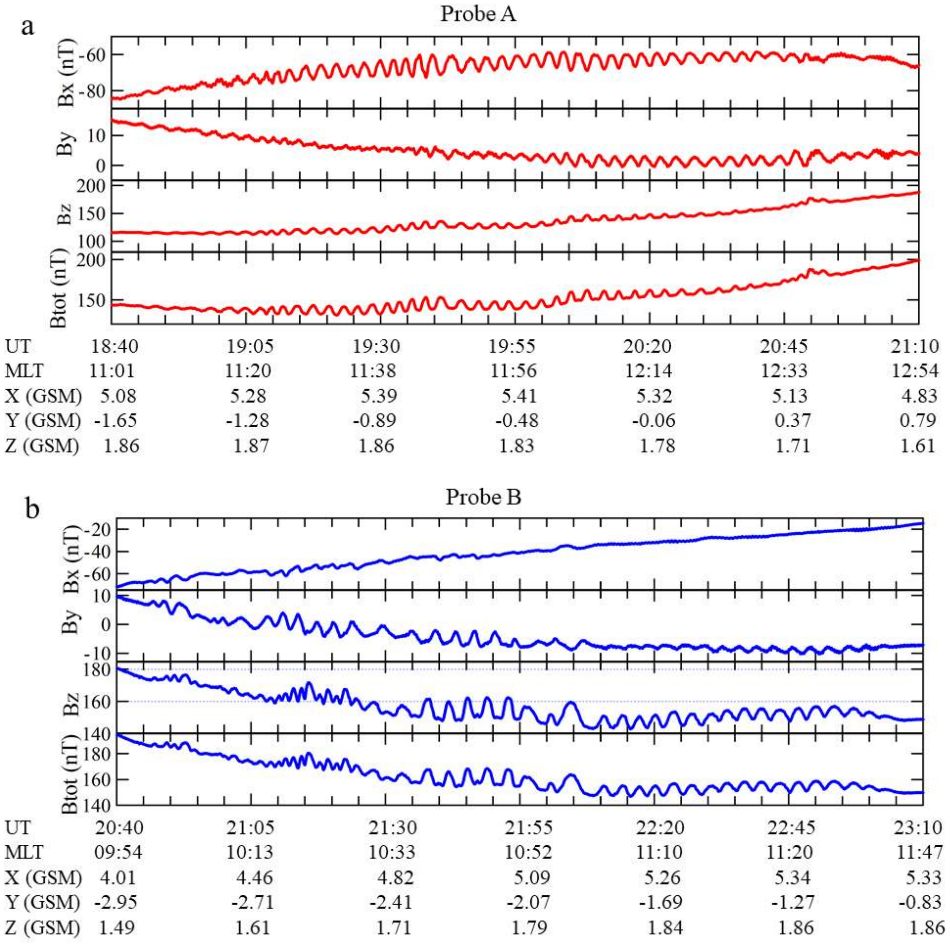

473

474

475 Figure 5. RBSP-A (a) and -B (b) magnetic field observations in GSM coordinates from 18:40
476 UT to 21:10 UT and from 20:40 UT to 23:10 UT on January 1, 2016, respectively. Beneath the
477 panels are listed the universal time (UT), magnetic local time (MLT), X (GSM). Y (GSM) and Z
478 (GSM) in Earth radii.

https://doi.org/10.5194/angeo-2020-32
Preprint. Discussion started: 26 June 2020

Annales Geophysicae Discussions
Open Access
EGU

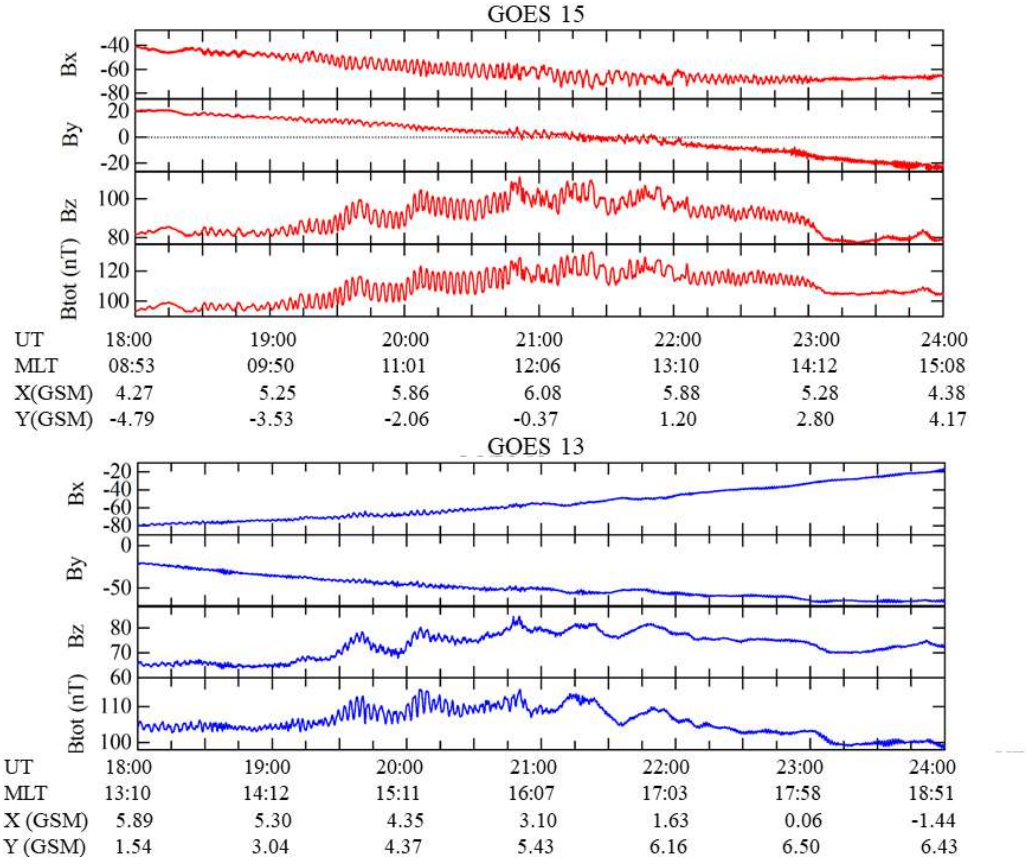

Figure 6. G-13 and 15 observations of the magnetic field in GSM coordinates from 18:00 UT to 24:00 UT on January 1, 2016. Beneath the panels are listed the universal time (UT), magnetic local time (MLT in SM), X (GSM) and Y (GSM) in Earth radii.

https://doi.org/10.5194/angeo-2020-32
Preprint. Discussion started: 26 June 2020

Annales Geophysicae Discussions
Open Access
EGU

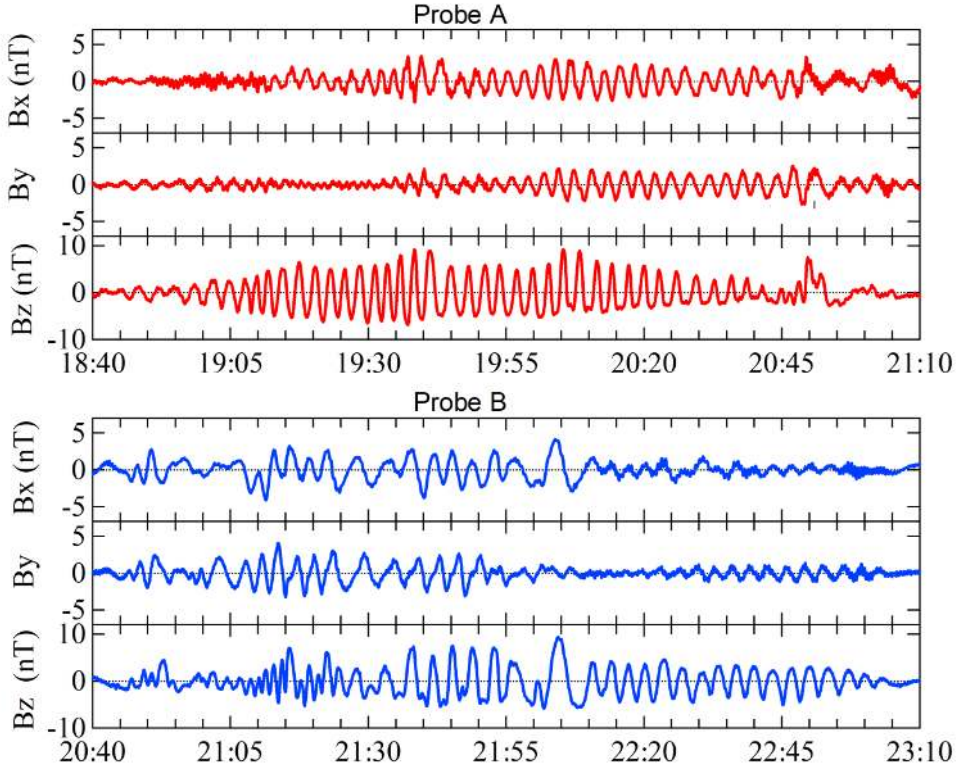

Figure 7. RBSP-A and -B magnetic field observations in field-aligned coordinates from 18:40 UT to 21:10 UT and from 20:40 UT to 23:10 UT on January 1, 2016, respectively.

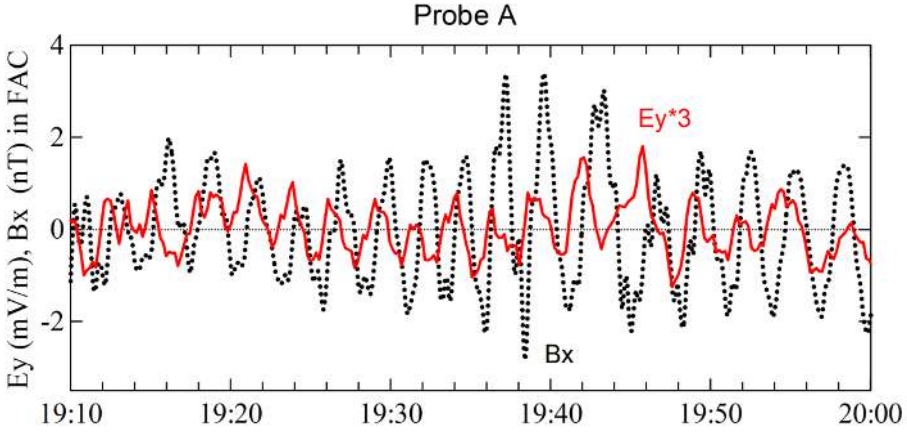

Figure 8. The phase difference between the RBSP-A azimuthal component of the electric field (red curve is boxcar smoothed) and the radial component of the magnetic field Bx in field-

https://doi.org/10.5194/angeo-2020-32
Preprint. Discussion started: 26 June 2020

Annales Geophysicae Discussions
Open Access
EGU

489 aligned coordinates (dashed curve) from 19:10 UT to 20:00 UT on January 1, 2016. The
490 amplitude of Ey was multiplied by a factor of 3 to better display the visual effects.

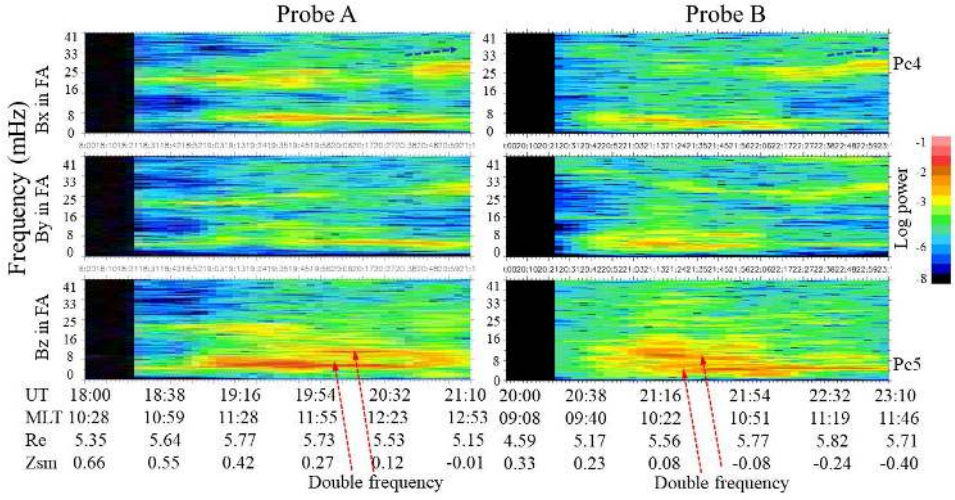

491

492 Figure 9. Three component dynamic spectra of magnetic field data at RBSP-A and -B from
493 18:00 to 21:10 UT and from 20:00 UT to 23:10 UT on January 1, 2016, respectively. Beneath
494 the panels are listed the universal time (UT), magnetic local time (MLT), radius (Re) and Z
495 (SM) in Earth radius.

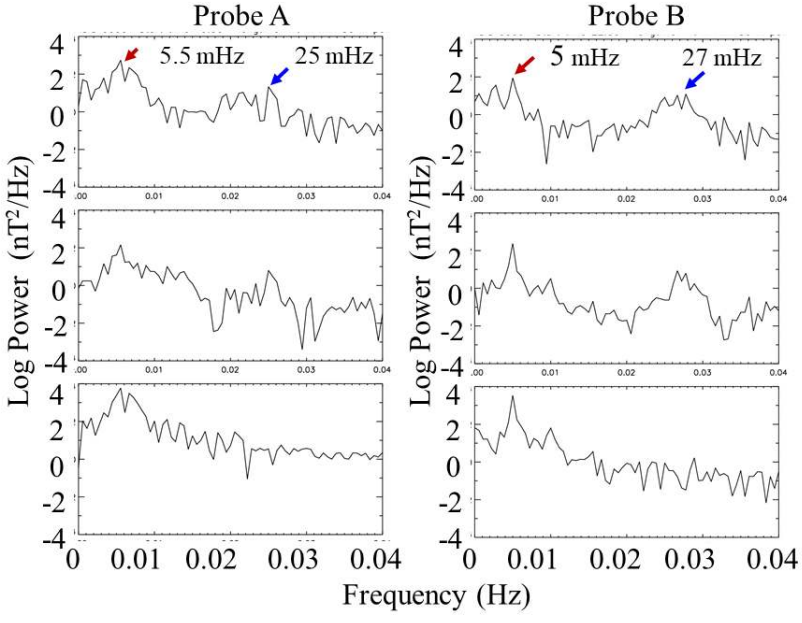

496

https://doi.org/10.5194/angeo-2020-32
Preprint. Discussion started: 26 June 2020

Annales Geophysicae Discussions
Open Access
EGU

497 Figure 10. Fourier spectra calculated for the radial, azimuthal and compressional components of
498 the RBSP-A and -B magnetic field in 5-minute sliding averaged mean field-aligned coordinates
499 from 19:30 UT to 20:00 UT and from 22:30 UT to 23:00 UT on 1 January, 2016.
500

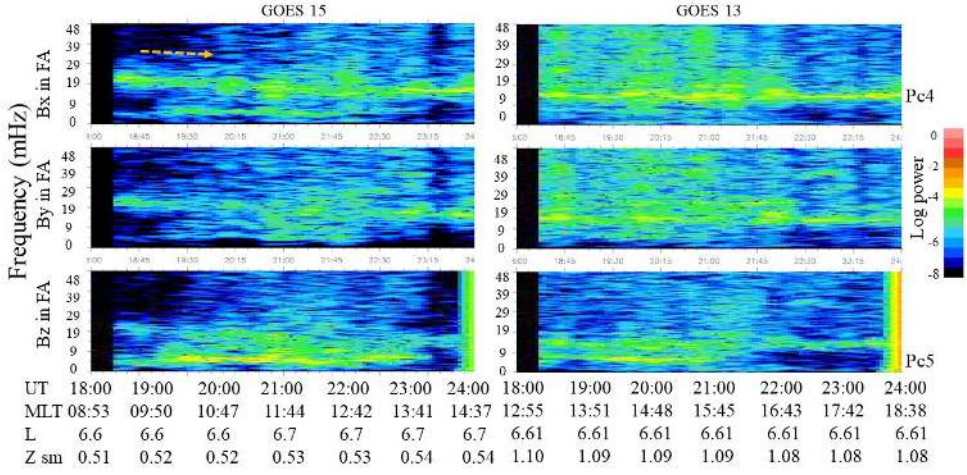

501
502 Figure 11. Three components of dynamic spectra of the magnetic field data at G-15 and G-13
503 from 18:00 UT to 24:00 UT on January 1, 2016. Beneath the panels are listed the universal
504 time (UT), magnetic local time (MLT in SM), L and Z (SM) in Earth radii.

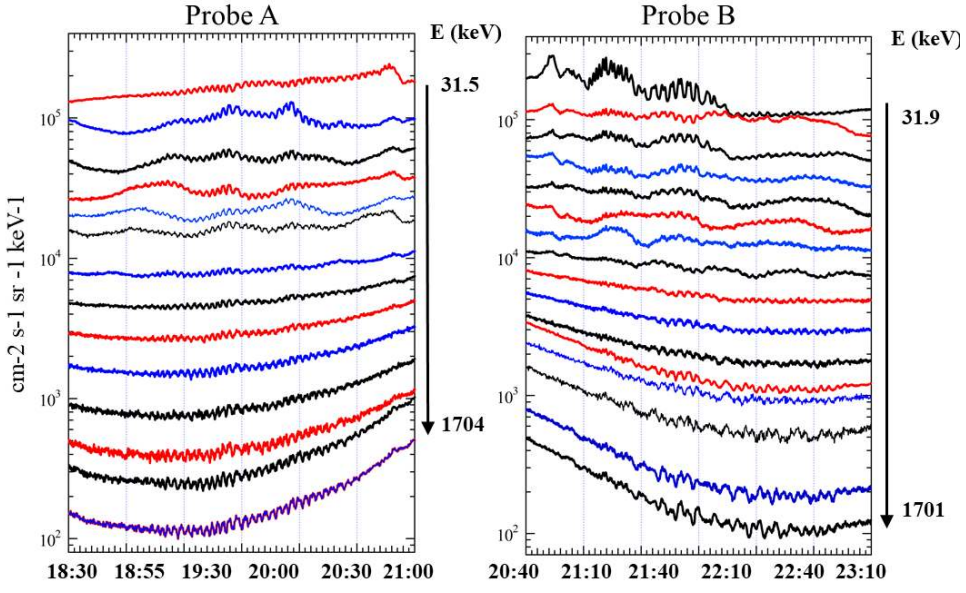

505

https://doi.org/10.5194/angeo-2020-32
Preprint. Discussion started: 26 June 2020

Figure 12. RBSP-A and -B observations of electron fluxes in the range of energies from 31.5 keV to 1704 keV from 18:30 UT to 21:00 UT and from 20:40 UT to 23:10 UT, respectively.

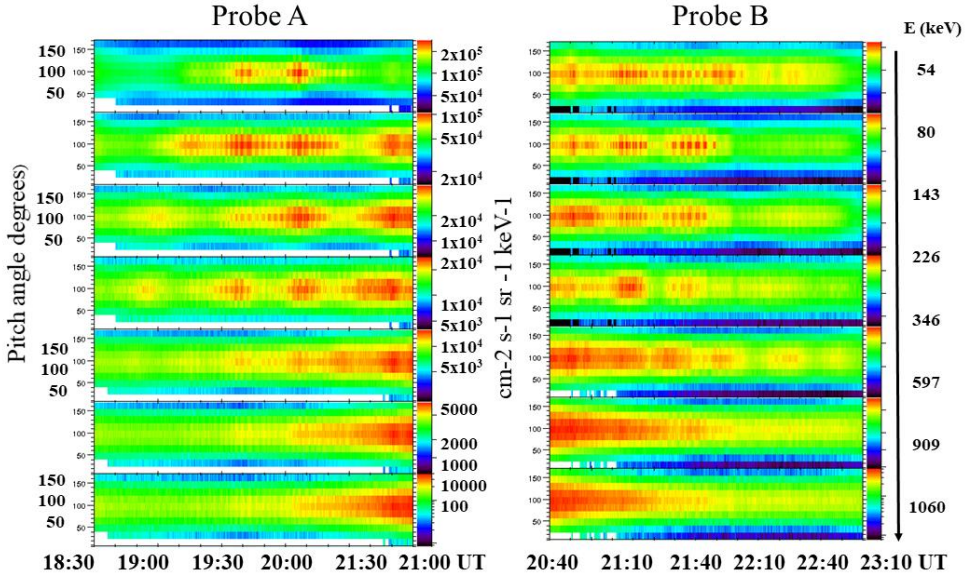

Figure 13. RBSP-A and -B observations of pitch-angle distributions for electrons in the range of energies from 54 keV and 1060 keV from 18:30 to 21:00 UT and from 20:40 UT to 23:10 UT on January 1, 2016, respectively.

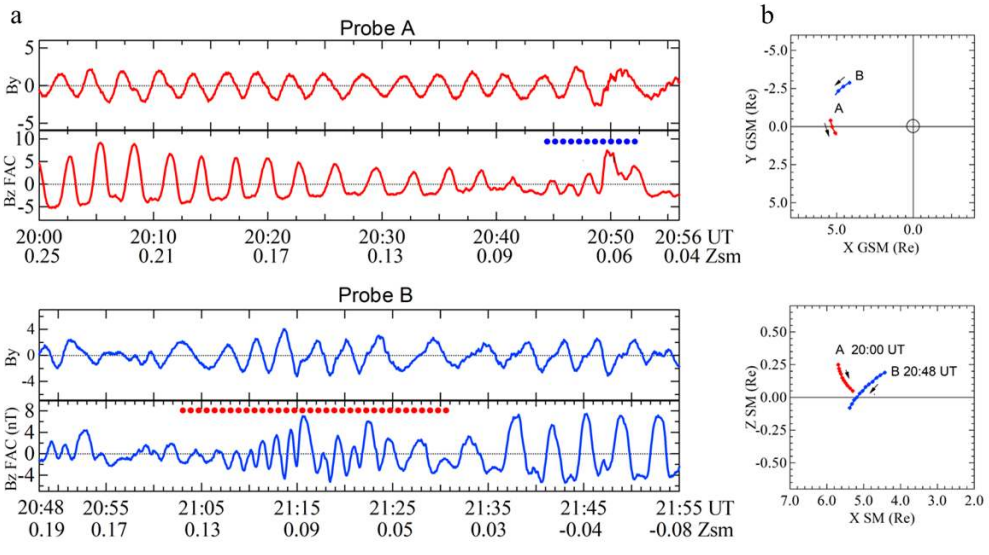

https://doi.org/10.5194/angeo-2020-32
Preprint. Discussion started: 26 June 2020

Annales Geophysicae Discussions
Open Access
EGU

513 Figure 14. RBSP-A and -B observations of double frequency pulsations (a) from 20:00 UT to
514 20:56 UT and from 20:48 UT to 21:55 UT, respectively, and (b) their locations in the X - Y
515 GSM and X - Z SM planes. Red and blue dashed lines mark the intervals with harmonic
516 structure of double-frequency pulsations.

517

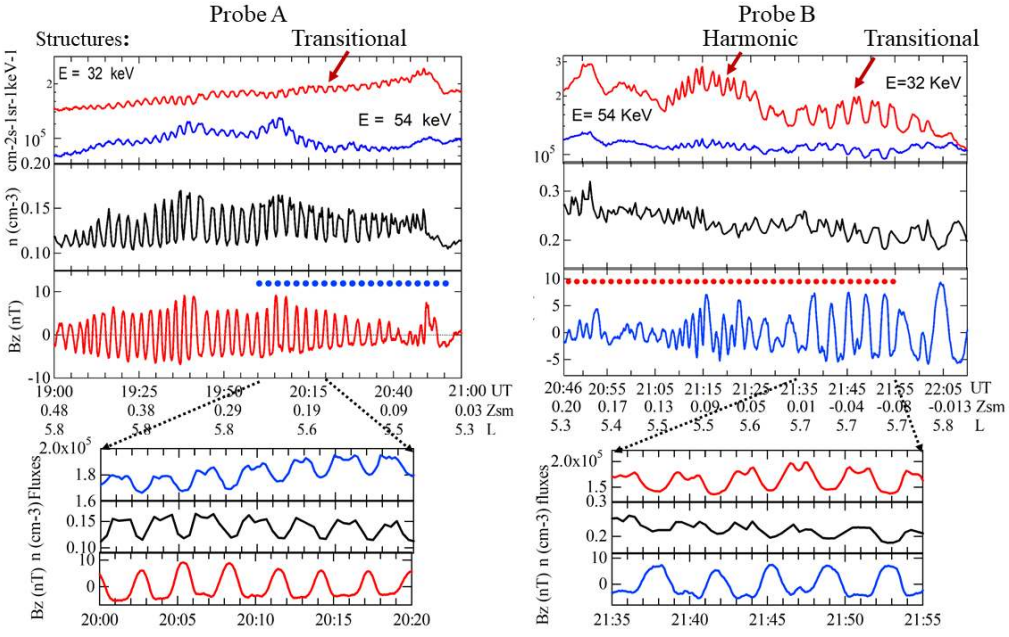

518
519

520 Figure 15. RBSP-A (left panel) and -B (right panel) presents electron fluxes for energies at
521 31.9 keV and 54.8 keV from EMFISIS, electron densities from HOPE and the Bz component
522 of the magnetic field in field-aligned coordinates from MagEIS from 19:00 UT to 21:00 UT and
523 from 20:46 UT to 22:10 UT, respectively. Dashed lines mark the intervals of observations of
524 double-frequency pulsations. The panels in the bottom of the figure present expanded views of
525 20 min intervals with the double-frequency pulsations to better visualize their features.

https://doi.org/10.5194/angeo-2020-32
Preprint. Discussion started: 26 June 2020

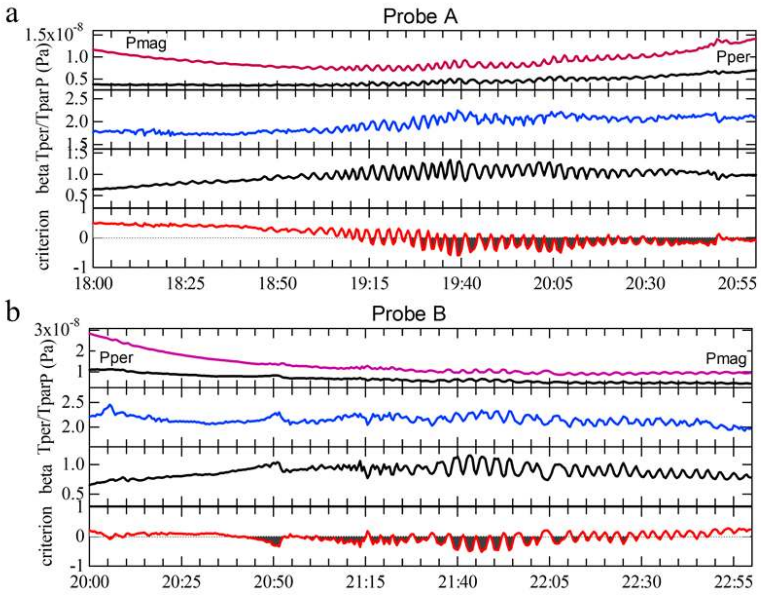

Figures 16a and b. RBSP-A and -B plasma and magnetic field parameters characterizing the pulsations. From top to bottom, the figure shows the magnetic pressure, perpendicular plasma pressure, the ratio of the plasma temperatures perpendicular and parallel to the magnetic field, beta, and the results for the mirror instability criterion on January 1, 2016. Shaded grey areas indicate the times when the drift mirror instability is satisfied (< 1).

Data availability. Data used in the paper are available publicly at http://cdaweb.gsfc.nasa.gov/istp_public/ (Coordinated Data Analysis Web, NASA, 2018). GOES data were obtained from http:// satdat.ngdc.noaa.gov/sem/goes/data/new_full/ (NOAA, 2018). The electric field data were obtained from http://www.space.umn.edu/ rbspefw-data (Wygant and Breneman, 2017).

Author contributions. GK drafted and wrote the paper with participation of all coauthors. DS conceived ideas, ME, ST, HS, CK –consulting regarding the data analysis, RR – software development, MB–consulting regarding drift mirror instability test.

Competing interests. The authors have no conflict of interest.

Acknowledgements. The Van Allen Probes mission is supported by NASA. NASA GSFC's CDAWEB provided Wind and GOES observations, while SSCWEB provided Van Allen Probes EPHEMERIS. GK was supported by NASA contract no 80NSSC19K0440. M. A. B. is grateful to the STFC (grant ST/R000697/1).

References

https://doi.org/10.5194/angeo-2020-32
Preprint. Discussion started: 26 June 2020

547 Blake, J. B., Carranza, P. A., Claudepierre, S. G., Clemmons, J. H., Crain Jr., W. R., Dotan, Y.,
548 Fennell, J. F., Fuentes, F. H., Galvan, R. M., George, J. S., Henderson, M. G., Lalic, M.,
549 Lin, A. Y., Looper, M. D., Mabry, D. J., Mazur, J. E., McCarthy, B., Nguyen, C. Q.,
550 O'Brien, T. P., Perez, M. A., Redding, M. T., Roeder, J. L., Salvaggio, D. J., Sorensen, G.
551 A., Spence, H. E., Yi, S., and Zakrzewski, M. P.: The Magnetic Electron Ion Spectrometer
552 (MagEIS) Instruments Aboard the Radiation Belt Storm Probes (RBSP) Spacecraft, Space
553 Sci. Rev., 179, 383–421, https://doi.org/10.1007/s11214-013-9991-8, 2013.

565 Chen, L., and Hasegawa, A.: Kinetic theory of geomagnetic pulsations.1. Internal excitations by
566 energetic particles, J. Geophys. Res., 96, 1503–1512, https://doi.org/10.1029/90JA02346,
567 1991.

568 Cheng, C. Z. and Lin, C. S.: Eigenmode analysis of compressional waves in the magnetosphere,
569 Geophys. Res. Lett., 8, 884–887, https://doi.org/10.1029/GL014i008p00884, 1987.

570 Cheng, C. Z., and Q. Qian, O.: Theory of ballooning-mirror mode instabilities for anisotropic
571 pressure plasmas in the magnetosphere, J. Geophys. Res., 99, 11,193–11,210.,
572 https://doi.org/10.1029/94JA00657, 1994.

573 Coleman Jr., P. J.: Geomagnetic storms at ATS 1, in: Intercorrelated Satellite observations
574 related to solar events, edited by: Manno V., Page D.E. (eds), Intercorrelated Satellite
575 Observations Related to Solar Events. Astrophysics and Space Science Library, vol 19.
576 Springer, Dordrecht, https://doi.org/10.1007/978-94-010-3278-0_18, 1970.

577 Constantinescu, O. D., Glassmeier, K.-H., Plaschke, F., Auster, U., Angelopoulos, V.,
578 Baumjohann, W., Fornaçon, K.-H., Georgescu, E., Larson. D., Magnes, W., McFadden,
579 J. P., Nakamura, R., Narita, Y.: THEMIS observations of dusk side compressional Pc 5
580 pulsations, J. Geophys. Res., 114, A00C25, doi:10.1029/2008JA013519, 2009.

581 Cummings, W.D., O'Sullivan, R.J., and Coleman Jr., P.J.: Standing Alfvén waves in the
582 magnetosphere, J. Geophys. Res., 74, 778 – 793, https://doi.org/10.1029/JA074i003p00778,
583 1969.

584 Dai, L., Takahashi, K., Wygant, J. R., Chen, L., Bonnell, J., Cattell, C. A., Thaller, S., Kletzing,
585 C., Smith, C. W., MacDowall, R.J, Baker, D.N., Blake, J. B., Fennell, J., Claudepierre,S.,
586 Funsten, H.O., Reeves, G.D., and Spence, H.E.: Excitation of poloidal standing Alfven
587 waves through drift resonance wave-particle interaction, Geophys. Res. Lett., 40, 4127–
588 4132, doi:10.1002/grl.50800, 2013.

589 Elkington, S. R., Hudson, M .K., and Chan, A. A.: Resonant acceleration and diffusion of outer
590 zone electrons in an asymmetric geomagnetic field, J. Geophys. Res., 108(A3), 1116,
591 doi:10.1029/2001JA009202, 2003.

https://doi.org/10.5194/angeo-2020-32
Preprint. Discussion started: 26 June 2020

592 Engebretson, M., Glassmeier, K.– H., Stellmacher, M., Hughes, W. J., Lühr, H.: The
593 dependence of high-latitude PcS wave power on solar wind velocity and on the phase of
594 high-speed solar wind streams, J. Geophys. Res., 103(A11), 26,271–26,283,
595 doi:10.1029/97JA03143, 1988.
596 Guo, X. C., Wang, C., and Hu, Y. Q.: Global MHD simulation of the Kelvin-Helmholtz
597 instability at the magnetopause for northward interplanetary magnetic field, J. Geophys.
598 Res., 115, A10218, doi:10.1029/2009JA015193, 2010.
599 Hedgecock, P. C.: Giant Pc5 pulsations in the outer magnetosphere: A study of HEOS-1 data,
600 Planet. Space Sci., 24, 921-935, https://doi.org/10.1016/0032-0633(76)90003-9, 1976.
601 Higbie, P.R., Baker, D.N., Zwickl, R.D., Bellian, R.D., Asbridge, J.R., Fennell, J.F., Wilken, B.,
602 and Arthur, C.W.: The Global Pc 5 Event of November 14–15, 1979, J. Geophys. Res., 87,
603 2337– 2345, https://doi.org/10.1029/JA087iA04p02337, 1982.
604 Higuchi, T., Kokubun, S., and Ohtani, S.: Harmonic structure of compressional Pc 5 pulsations
605 at synchronous orbit, Geophys. Res. Lett., 13, 1101,
606 https://doi.org/10.1029/GL013i011p01101, 1986.
607 Kepko, L., and Spence, H. E.: Observations of discrete, global magnetospheric oscillations
608 directly driven by solar wind density variations, J. Geophys. Res., 108, 1257,
609 doi:10.1029/2002JA009676, 2003.
610 Kivelson, M. G. and Southwood, D. J.: Charged particle behavior in low-frequency geomagnetic
611 pulsations, 4. Compressional waves, J. Geophys. Res., 90, 1486–1498,
612 https://doi.org/10.1029/JA090iA02p01486, 1985.
613 Kletzing, C. A., Kurth, W. S., Acuna, M., MacDowall, R. J., Torbert, R. B., Averkamp, T.,
614 Bodet, D., Bounds, S. R., Chutter, M., Connerney, J., Crawford, D., Dolan, J. S., Dvorsky
615 R., Hospodarsky, G. B., Howard, J., Jordanova, V., Johnson, R. A., Kirchner, D. L.,
616 Mokrzycki, B., Needell, G., Odom, J., Mark, D., Pfaff Jr., Phillips, J. R., Piker, C. W.,
617 Remington, S. L., Rowland, D., Santolik, O., Schnurr, R., Sheppard, D., Smith, C. W.,
618 Thorne, R. M., and Tyler, J.: The Electric and Magnetic Field Instrument Suite and
619 Integrated Science (EMFISIS) on RBSP, Space Sci. Rev., 179, 127–181,
620 doi:10.1007/s11214-013-9993-6, 2013.
621 Korotova, G. I., Sibeck, D. G., Angelopoulos, V., and Walsh, W.: Themis observations of
622 compressional poloidal pulsations in the dawnside magnetosphere: a case study, J. Geophys.
623 Res., 118, 7665–7673, doi:10.1002/2013JA019360, 2013.
624 Kokubun, S., Statistical characteristics of Pc 5 waves at geostationary orbit, J. Geomag.
625 Geoelectr., 37, 759–779, https://doi.org/10.5636/jgg.37.759, 1985.

https://doi.org/10.5194/angeo-2020-32
Preprint. Discussion started: 26 June 2020

626 Kremser, G., Korth, A., Feier, J. A., Wilken, B., Gurevich, A. V., and Amata, E.: Observations
627 of quasi-periodic flux variations of energetic ions and electron associated with Pc5
628 geomagnetic pulsations, J. Geophys. Res., 86, 3345–3356,
629 https://doi.org/10.1029/JA086iA05p03345, 1981.
630 Lanzerotti, L. J., Hasegawa, A., and Maclennan, C. G.: Drift mirror instability in the
631 magnetosphere: Particle and field oscillations and electron heating, J. Geophys. Res., 74,
632 5565–5578, https://doi.org/10.1029/JA074i024p05565, 1969.
633 Lin, C. S., Parks, G. K., and Winckler J. R.: The 2-to12-min quasi-periodic variation of 50-to
634 1000-keV trapped electron fluxes, J. Geophys. Res., 81(25),4517–4523,
635 https://doi.org/10.1029/JA081i025p04517, 1976.
636 Lin, C. S. and Parks, G. K.: The coupling of Alfven and compressional waves, J. Geophys. Res.,
637 83, 2628–2636, https://doi.org/10.1029/JA083iA06p02628, 1978.
638 Liu, H., Zong, Q.-G., Zhou, X. Z., Fu, S. Y., Rankin, R., Wang, L.-H., Yuan C. J., Wang, Y. F.,
639 Baker, D. N., Blake, J. B., and Kletzing, C. A. : Compressional ULF wave modulation of
640 energetic particles in the inner magnetosphere. Journal of Geophysical Research: Space
641 Physics, 121, 6262–6276, https://doi.org/10.1002/ 2016JA022706, 2016.
642 Lin, R. P., Anderson, K. A., Ashford S., Carlson, C., Curtis, D., Ergun, R., Larson, D.,
643 McFadden, J., McCarthy, M., Parks, G. K., Rème, H., Bosqued, J. M., Coutelier, J.,
644 Cotin, F., Wenzel, K.-P., Sanderson, T. R., Henrion, J., Ronnet, J. C., Paschmann, G.: A
645 three-dimensional (3-D) plasma and energetic particle experiment for the Wind spacecraft of
646 the ISTP/GGS mission, Space Sci. Rev.,71, 125–153, https://doi.org/10.1007/BF00751328,
647 1995.
648 Lepping, R.P., Acuna, M.H., Burlaga, L.F., Farrell, W.M., Slavin, J. A., Schatfen, K. H.,
649 Mariani, E., Ness, N. E., Neubauer, E. M., Whang, Y. C., Byrnes J. B., Kennon R. S.,
650 Panetta, P. V., Scheifele J., and Worley, E. M.: The WIND Magnetic field investigation,
651 Space Sci. Rev., 71, 207–229, https://doi.org/10.1007/BF00751330, 1995.
652 Mauk, B. H., Fox, N. J., Kanekal, S. G., Kessel, R. L., Sibeck, D. G., and Ukhorskiy, A.: Science
653 objectives and rationale for the radiation belt storm probes mission, Space Sci. Rev., 179, 3–
654 27, doi:10.1007/s11214-012-9908-y, 2012.
655 Motoba, T., Kikuchi, T., Okuzawa, T., and Yumoto, K.: Dynamical response of the
656 magnetosphere-ionosphere system to a solar wind dynamic pressure oscillation, J. Geophys.
657 Res., 108(A5), 1206, doi:10.1029/ 2002JA009696, 2003.
658 Nagano, H. and Araki, T.: Long-duration Pc5 pulsations observed by geostationary satellites,
659 Geophys. Res. Lett., 10, 908–911, https://doi.org/10.1029/GL010i009p00908, 1983.

https://doi.org/10.5194/angeo-2020-32
Preprint. Discussion started: 26 June 2020

660 NASA: Coordinated Data Analysis Web, available at: http:// cdaweb.gsfc.nasa.gov/istp_public/,
661 last access: 1 March 2020.
662 NOAA: GOES SEM fata, available at: http://satdat.ngdc.noaa.gov/ sem/goes/data/new_full/, last
663 access: 2 January 2019.
664 Pokhotelov, O. A., Pilipenko,V. A., Nezlina, I. M., Woch, J., and Kremser, G.: Excitation of
665 high β plasma instabilities at the geostationary orbit: Theory and observations, Planet. Space
666 Sci., 34, 695–712, https://doi.org/10.1016/0032-0633(86)90124-8,1986.
667 Samson, J. C., Harrold, B. G., Ruohoniemi, J. M., Greenwald, R. A., and Walker, A. D. M.:
668 Field line resonance associated with MHD waveguides in the magnetosphere, Geophys. Res.
669 Lett., 19, 441–444, https://doi.org/10.1029/92GL00116, 1992.
670 Sarris, T.E., Liu, W., Li, X., Kabin, K., Talaat, E.R., Rankin, R., Angelopoulos, V.,
671 Bonnell, J., Glassmeier, K.-H.: THEMIS observations of the spatial extent and
672 pressure-pulse excitation of field line resonances, Geophys. Res. Lett., 37, L15104,
673 https://doi.org/10.1029/2010GL044125, 2010.
674 Singer, H.J., Matheson, L., Grubb, R., Newman, A., and Bouwer, S. D.: Monitoring space
675 weather with the GOES magnetometers, in: SPIE Conference Proceedings, vol. 2812, edited
676 by: Washwell, E. R., 299–308, GOES-8 and Beyond SPIE, Bellingham, WA, USA, 1996.
677 Shen, X.-C., Shi, Q., Wang, B., Zhang, H., Hudson, M. K., Nishimura, Y., Hartinger, M. D.,
678 Tian, A., Zong, Q_G., Rae, I. J., and Degeling, A. W.: Dayside magnetospheric and
679 ionospheric responses to a foreshock transient on 25 June 2008: 1. FLR observed by satellite
680 and ground-based magnetometers. Journal of Geophysical Research: Space Physics, 123,
681 6335–6346. https://doi.org/10.1029/2018JA025349, 2018.
682 Southwood, D. J., Dungey, J. W., and Etherington, R. J.: Bounce resonance interaction between
683 pulsations and trapped particles, Planet. Space Sci., 17, 349–361,
684 https://doi.org/10.1016/0032-0633(69)90068-3, 1969.
685 Southwood, D. J.: The behaviour of ULF waves and particles in the magnetosphere, Planet.
686 Space Sci., 21, 53–65, https://doi.org/10.1016/0032-0633(73)90019-6, 1973.
687 Southwood D.J.: Low Frequency Pulsation Generation by Energetic Particles, Advances in
688 Earth and Planetary Sciences, vol 11. Springer, Dordrecht,
689 https://doi.org/10.1007/978-94-009-8426-4_5, 1981.
690 Southwood, D. J. and Kivelson, M. G.: Mirror instability: 1. Physical mechanism of linear
691 instability, J. Geophys. Res., 98, 9181– 9187, https://doi.org/10.1029/92JA02837, 1993.
692 Spence, H. E., Reeves, G. D., Baker, D. N., Blake J. B., Bolton, M., Bourdarie, S., Chan, S. G.
693 Claudpierre, S. G., Clemmons, J. H., Cravens, J. P., Elkington, S. R., Fennell, J. F., Friedel,

https://doi.org/10.5194/angeo-2020-32
Preprint. Discussion started: 26 June 2020

694 R. H. W., Funsten, H. O., Goldstein, J., Green, J. C., Guthrie, A., Henderson, M. G., Horne,
695 R. B., Hudson, M. K., Jahn, J.-M., Jordanova, V. K., Kanekal, S. G., Klatt, B. W., Larsen, B.
696 A., Li, X., MacDonald, E. A., Mann, I. R., Niehof, J., O'Brien, T. P., Onsager, T. G.,
697 Salvaggio, D., Skoug, R. M., Smith, S. S., Suther, L. L., Thomsen, M. F., and Thorne R. M.:
698 Science goals and overview of the Energetic Particle, Composition, and Thermal Plasma
699 (ECT) Suite on NASA's Radiation Belt Storm Probes (RBSP) Mission, Space Sci. Rev.,
700 179, 311–336, doi:10.1007/s11214013-0007-5, 2013.
701 Sugiura, M., and Wilson, C. R.: Oscillation of the geomagnetic field lines and associated
702 magnetic perturbations at conjugate points, J. Geophys. Res., 69, 1211–1216,
703 https://doi.org/10.1029/JZ069i007p01211, 1964.
704 Takahashi, K., McPherron, R. L., Hughes, W. J.: Multispacecraft observations of the harmonic
705 structure of Pc 3–4 magnetic pulsations, J. Geophys. Res., 89, 6758-6774,
706 https://doi.org/10.1029/JA089iA08p06758, 1984.
707 Takahashi, K., Higbie, P. R., and Baker, D. N.: Azimuthal propagation and frequency
708 characteristic of compressional Pc 5 waves observed at geostationary orbit, J. Geophys.
709 Res., 90, 1473– 1485, https://doi.org/10.1029/JA090iA02p01473, 1985.
710 Takahashi, K., and Higbie, P. R.: Antisymmetric standing wave structure associated with the
711 compressional Pc 5 pulsation of November 14, 1979, J. Geophys. Res., 91, 11163–11178,
712 https://doi.org/10.1029/JA091iA10p11163, 1986.
713 Takahashi, K., Fennell, J. F., Amata, E., Higbie, P. R.: Field-aligned structure of the storm time
714 Pc5 wave of November 14–15, 1979, J. Geophys. Res., 92, 5857–5864,
715 https://doi.org/10.1029/JA092iA06p05857, 1987a.
716 Takahashi, K., L. J. Zanetti, T. A. Potemra, and M. H. Acuña: A model for the harmonic of
717 compressional Pc5 waves, Geophys. Res. Let., 14, 363–366,
718 https://doi.org/10.1029/GL014i004p00363, 1987b.
719 Takahashi, K., Cheng, C. Z., McEntire, R. W., and Kistler, L. M.: Observation and theory of Pc5
720 waves with harmonically related transverse and compressional components, J. Geophys
721 Res., 95, 977–989, https://doi.org/10.1029/JA095iA02p00977, 1990.
722 Takahashi, K., Glassmeier, K.-H., Angelopoulos, V., Bonnell, J., Nishimura, Y., Singer, H.
723 J., and Russell, C. T.: Multisatellite observations of a giant pulsation event, J. Geophys.
724 Res., 116, A11223, doi:10.1029/2011JA016955, 2011.
730 Vaivads, A., Baumjohann, W., Haerendel, G., Nakamura, R., Kucharek, H., Klecker, B.,
731 Lessard, M.R., Kistler, L. M., Mukai, T., and A. Nishida, A: Compressional Pc5 type

https://doi.org/10.5194/angeo-2020-32
Preprint. Discussion started: 26 June 2020

732 pulsations in the morning plasma sheet, Ann. Geophys., 19, 311–320,
733 https://doi.org/10.1029/2001JA900042, 2001.
734 Walker, A. D. M., Greenwald, R. A., Korth, A., Kremser, G.: STARE and GEOS 2 observations
735 of a storm time Pc5 ULF pulsation, J. Geophys. Res., 87, 9135–9146,
736 https://doi.org/10.1029/JA087iA11p09135, 1982.
737 Wang, B., Nishimura, Y., Hietala, H., Shen, X.-C., Shi, Q., Zhang, H., Lyons. L., Zou, Y.,
738 Angelopoulos, V., Ebihara, Y., Weatherwax, A.: Dayside magnetospheric and ionospheric
739 responses to a foreshock transient on 25 June 2008: 2. 2-D evolution based on dayside
740 auroral imaging. Journal of Geophysical Research: Space Physics, 123, 6347–6359.
741 https://doi.org/10.1029/2017JA024846, 2018.
742 Zhang, X. Y., Zong, Q.-G., Wang, Y. F., Zhang, H., Xie, L., Fu, S. Y., Yuan, C. J., Yue, C.,
743 Yang, B., and Pu, Z. Y.: ULF waves excited by negative/positive solar wind dynamic
744 pressure impulses at geosynchronous orbit, J. Geophys. Res., 115, A10221,
745 https://doi:10.1029/2009JA015016, 2010.
746 Zhu, X. M. and Kivelson, M. G.: Compressional ULF waves in the outer magnetosphere: 1.
747 Statistical study. J. Geophys. Res., 96, 19451–19467, https://doi.org/10.1029/91JA01860,
748 1991.
749